Chinese Chemical Letters 36 (2025) 110294

Contents lists available at ScienceDirect

Chinese Chemical Letters

journal homepage: www.elsevier.com/locate/cclet

Nitrogen-containing linkage-bonds in covalent organic frameworks: Synthesis and applications

Liying Ou[a], Zhenluan Xue[a], Bo Li[a,*], Zhiwei Jin[a], Jiaochan Zhong[b], Lixia Yang[b], Penghui Shao[b,*], Shenglian Luo[b]

[a] School of Materials Science and Engineering, Nanchang Hangkong University, Nanchang 330063, China
[b] Key Laboratory of Jiangxi Province for Persistent Pollutants Prevention Control and Resource Reuse, Nanchang Hangkong University, Nanchang 330063, China

ARTICLE INFO

Article history:
Received 27 February 2024
Revised 25 June 2024
Accepted 24 July 2024
Available online 25 July 2024

Keywords:
Covalent organic frameworks
Nitrogen-containing linkage-bonds
Structure and properties
Synthesis strategy and application
Porous materials

ABSTRACT

Covalent organic frameworks (COFs) are crystalline porous polymeric materials composed of organic monomers connected by strong covalent bonds and offer high stability, good crystallinity, a large specific surface area, and controllable structures. COFs are widely used in the fields of adsorption and separation, catalysis, photovoltaics, and drug-delivery. The structural regulation and performance optimization of COFs can be realized through the modification of ligands and the selection of linkage methods. In which, the types of linkage are closely related to the stability and performance of COFs. In this review, nitrogen-containing linkage-bonds (NCLBs) in COFs are divided into N-containing double bonds, N-containing conjugated rings and N-containing unconjugated rings. The association between structure and performance of COFs is elaborated and the synthesis methods of COFs are systematically summarized. Moreover, the structural design, theoretical prediction and machinable application of COFs are prospected

1. Introduction

COFs are a class of organic, porous crystalline materials composed of light elements (*e.g.*, C, O, N, and B) connected by covalent bonds. COFs have been in public view since Yaghi published his initial study in 2005 [1]. In less than two decades, COFs have emerged as highly desirable materials owing to its exceptional crystallization properties, low density, large specific surface area, and remarkable structural designability. Therefore, they possess great application potential in molecular adsorption and separation [2], catalysis [3], sensing [2,4], energy storage [5], drug-delivery [6], *etc*.

Generally, the synthesis of covalent bonds in COFs is reversible [7], which contributes to optimize the structure of COFs and repair defects, thus forming a highly ordered framework structure. COFs formed by combining monomers with different shapes can be categorized as two-dimensional (2D) and three-dimensional (3D) COFs. According to the shape of stacked units, 2D COFs are further divided into triangles, quadrilaterals, pentagons, and hexagons [8].

COFs belong to crystalline polymers, in which monomers are linked by specific dynamic covalent bonds to form a lattice structure. Among the many linkages in the COFs, nitrogen-containing linkage-bonds (NCLBs) develop rapidly because of its easy synthesis, excellent environment stability, great coordination and catalysis.

In this review, the common COFs with NCLBs are classified into three types, including carbon/nitrogen-nitrogen double bonds, N-containing conjugated rings and N-containing unconjugated rings. The corresponding synthesis methods (Tables S1-S8 in Supporting information) and applications are expounded. Additionally, the cultivation methods of single crystals COFs (scCOFs) are briefly summarized, and the CCDC numbers of common scCOFs are provided (Table S9 and Fig. S1 in Supporting information), and the development of COFs is prospected.

2. Classification of NCLBs in COFs

With cross-disciplinary interaction and integration, various types of COFs structures and connection methods are developed to meet different application requirements. Currently, NCLBs in COFs primarily include C=N, N=N and imidazole. We categorize these bonds into three groups based on structural commonality (Fig. 1) and summarize the general equations of the COFs synthesis (Ar,

* Corresponding authors.
E-mail addresses: libochem@nchu.edu.cn (B. Li), penghui_shao@163.com (P. Shao).

https://doi.org/10.1016/j.cclet.2024.110294
1001-8417/

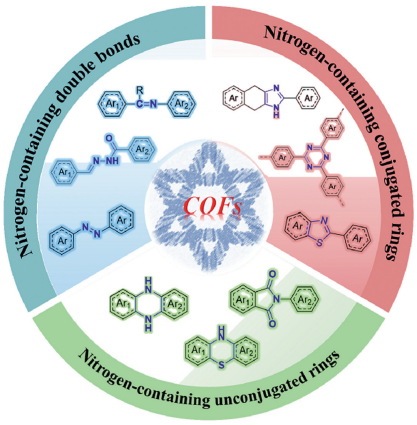

Fig. 1. Classification of NCLBs in COFs.

Ar_1 and Ar_2 represent different aromatic ligands, R, R_1, R_2 represent different substituents).

2.1. COFs based on N-containing double bonds linkage units

2.1.1. Imine-linked units

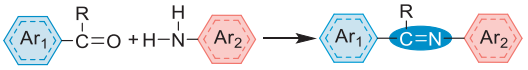

(1)

An imine bond (C=N) is primarily formed through the Schiff base condensation reaction between aldehydes (or ketones) and amines (or ammonia), catalyzed by acid (Eq. 1). Most imine-linked COFs, such as JUC-641 [9], NI-COF-1 [10], and DAA-TFPT-COF [11], were synthesized using acetic acid as the catalyst under solvothermal conditions (Table S1). The synthetic methods of these COFs are similar and have a certain reference value. Moreover, the synthesis of aldehyde and amine monomers is relatively straightforward, which contributes to the rapid development of this kind COFs materials over the past two decades. Currently, COFs are mainly connected by imine bonds, and the imine-linked COFs account for more than 60% of the total COFs [12]. Imine-linked COFs with a variety of structures and exceptional crystallinity have been explored extensively in both 2D and 3D COFs. They are widely used in various fields, including organic catalysis, adsorption and separation, photocatalysis, and sensor.

Most of imine-linked COFs focus on elucidating structure-function relationship, and excellent properties can be obtained by introducing different chemical groups into the structure. For example, pyridine groups can improve the adsorption and recovery abilities of Hg^{2+} in wastewater [13], and changing the orientation of imine bonds can significantly alter the photophysical and electrochemical properties of COFs [14]. At present, the study of imine-linked COFs has gradually focused on the regulation of ligand conformation, which extends from the original planar 2D network to the 3D framework. For example, drawing inspiration from the torsion phenomenon observed in 2D planar molecules, Cheng *et al.* synthesized a highly crystalline 3D-An-COF by incorporating anthracene units to form steric hindrance in the vertical direction [15]. Due to the absence of $\pi\cdots\pi$ interactions, anthracene units were exposed to the pore structure. 3D-An-COF exhibited distinct yellow fluorescent emission under ultraviolet (UV) light excitation, which can be utilized as a sensor to detect trace amounts of antibiotics in aqueous environments. Fang *et al.* synthesized 3D COFs (JUC-641 and JUC-642) with nia nets by using planar hexagonal and triangular prism nodes [9]. Both COFs had high crystallinity and can maintain abundant pores in strong acidic and alkaline environments. The separation factor of JUC-642 for benzene and cyclohexane was as high as 2.02, which exceeds the previously reported 3D COFs (Fig. 2a). It indicates that the COFs can be further optimized and developed by studying the structure and properties.

To date, a wide range of organic ligands with various functional groups have been designed (Fig. 2b) to satisfy the requirements for regulating the properties of materials. For example, molecules with donor-acceptor (D-A) properties, such as 4,7-diphenylbenzo[*c*][1,2,5] thiadiazole [16], 4,4′,4″,4‴-(benzo[*c*][1,2,5]thiadiazole-4,7-diylbis(9,9-dimethyl-9,10-dihydroacridine-10,2,7-triyl))tetrabenzaldehyde [17] and pyrene-based monomers [18], were used to construct photocatalytic hydrogen evolution monomers. And heterotriangulenes were used to enhance charge-carrier mobility [19]. It is worth noting that certain molecules can serve multiple roles as monomers. An *et al.* synthesized the COFs utilizing four (4-methylphenyl)vinyl units as monomers, which exhibited catalytic capabilities for 2e oxygen reduction reaction (ORR) [20]. You *et al.* demonstrated the great potential of COFs based on tetraphenylethylene in tumor cell imaging and therapy through its aggregation-induced emission properties [21]. Additionally, molecules with distorted conformations, such as tetra-phenylmethane [22] and saddle-shaped cyclooctatetrathiophene [23], and organic monomers with cage-like structures [24], were used to construct 3D COFs. However, currently, the structure of ligands cannot predict the folding and interlayer arrangement of COFs accurately [25], and the unique nonplanar spatial assembly further complicates synthesis procedures. Even though imine-linked COFs have surpassed other categories in terms of quantity, there is still ample room for exploration.

In addition, imine bond is an important chemical intermediate, which is widely used in organic materials synthesis and drug synthesis. Provided that the framework structure of the COFs remains stable, the imine bond can be transformed into other types of linkage bonds, such as amide bond [26], C–N bond [27], azo bond [28], quinolone [29,30], azoles [31,32] and other cyclic connecting units (Fig. 2c). In 2018, Li *et al.* demonstrated that imine-linked COF-1 can be transformed into quinoline-linked MF-1 by aza-Diels-Alder cycloaddition reaction. Cyclic quinoline improved the stability of the structure, and can effectively adjust the π electron delocalization, thus enhancing the photoelectric performance of the imine bonds [30]. In addition, these aromatic rings exposed to the pore can further meet the design requirements of some specific properties. Thus, many studies adopted "4 + 2 cycloaddition" reaction to further transform imine bonds. In 2024, Zhao *et al.* demonstrated that imine-linked Im-COF-TFPPy-PDA can be converted into azine-linked Py-azine COF by monomer exchange. The first fused BF-COFs linked with bicyclic-fused-ring was obtained by Criss-Cross [3 + 2] cycloaddition [33]. This strategy realized the transformation of the linking bond from linear to cyclic structure, which makes the structure of COFs on longer limited to direct synthesis or monomers conversion.

2.1.2. Azo-linked units

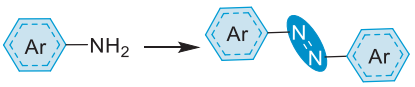

(2)

The methods of introducing azo bonds into COFs are few due to the low reversibility and difficulty of azo bond synthesis reaction [28]. Here, three methods of introducing azo bonds into COFs are summarized as follows:

Firstly, azo-linkage can be obtained by catalyzing the coupling reaction of amines group (Eq. 2). In 2021, Wu *et al.* prepared

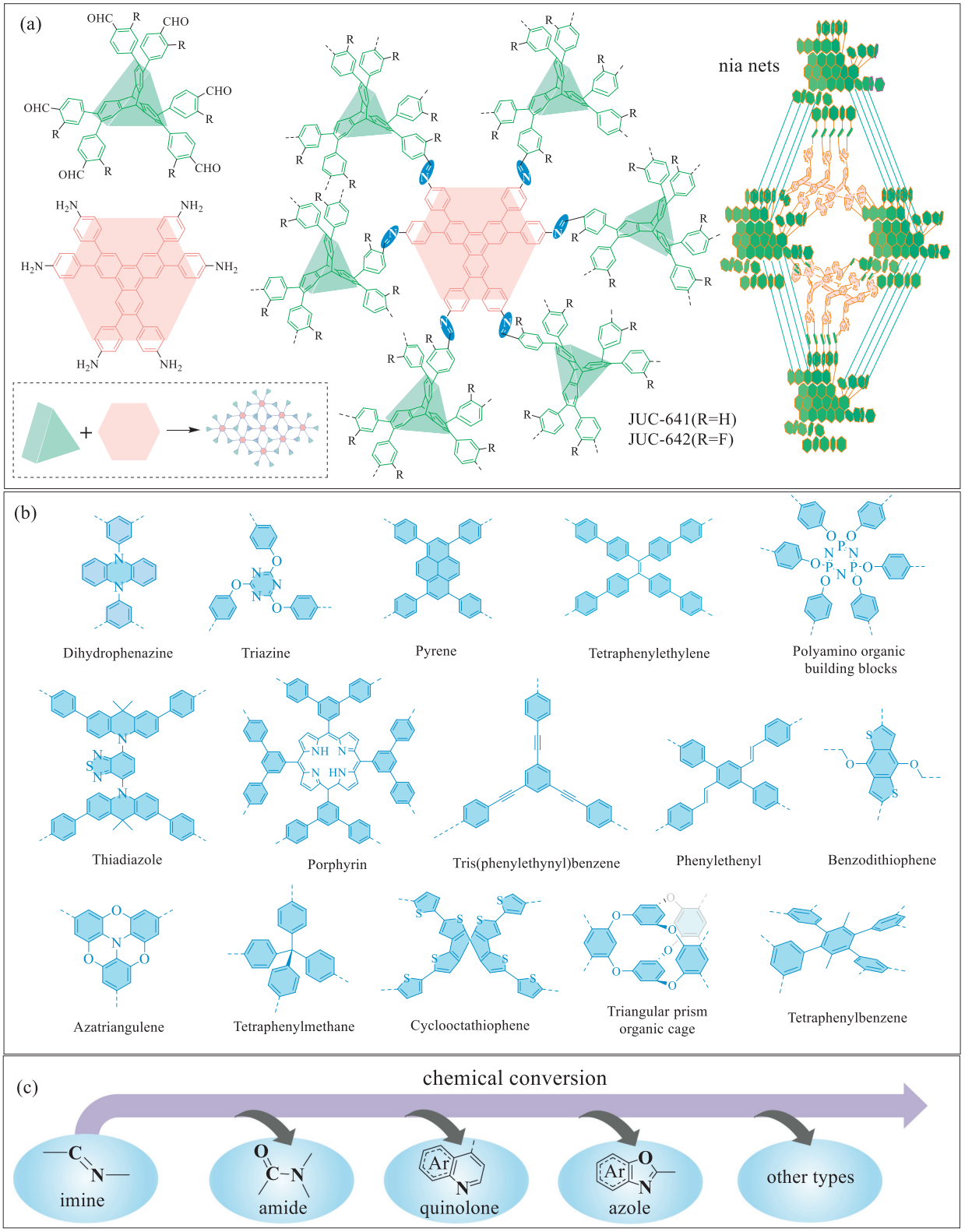

Fig. 2. (a) Two 3D COFs (JUC-641 and JUC-642) with the nia topology were constructed by introducing planar hexagonal and triangular prism nodes. Reproduced with permission [9]. Copyright 2024, Springer Nature. (b) Lots of organic ligands with various functional groups were designed for adjusting performance. (c) Imide-linked COFs were transformed into other types by chemical conversation of the linkage bond.

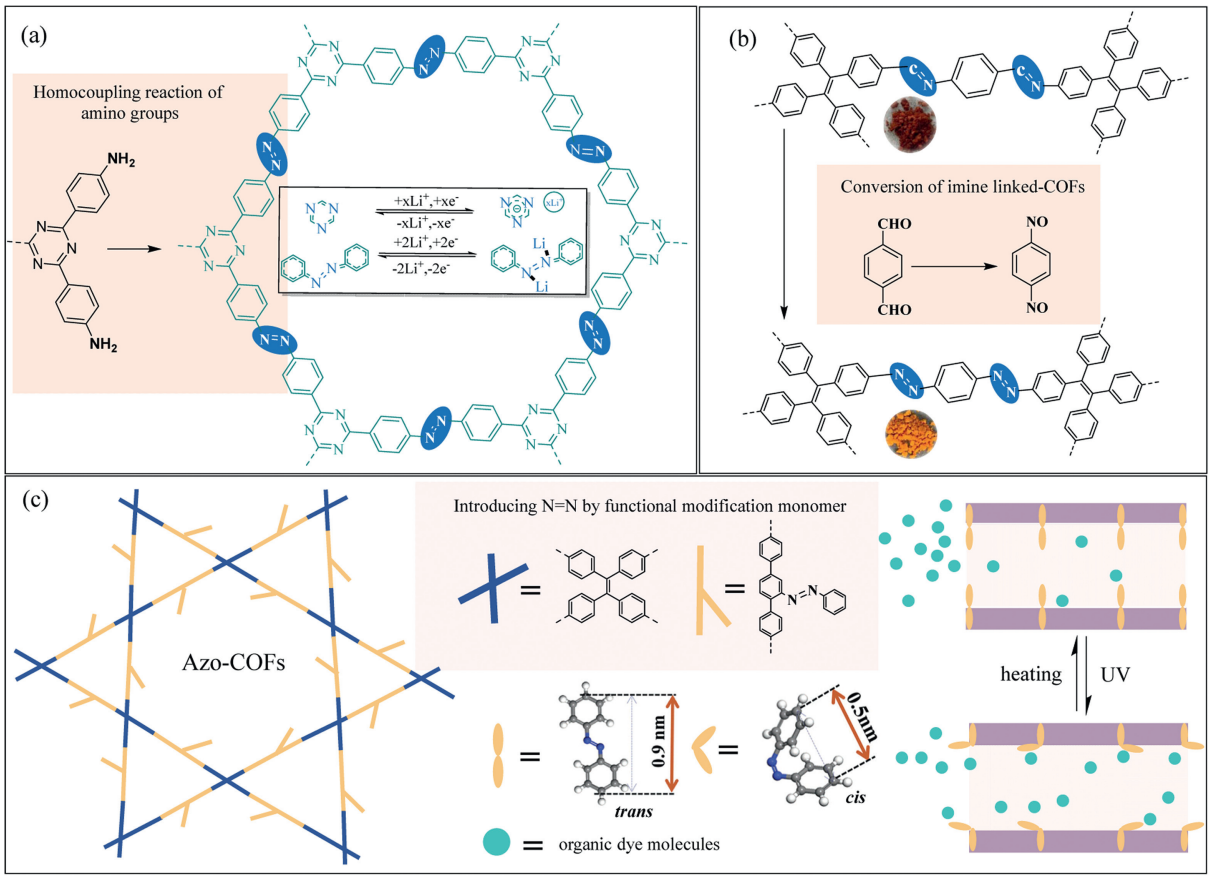

Fig. 3. (a) The azo linkage-bond was obtained by homocoupling reaction of amino group, which co-stores lithium with nitrogen-rich triazine. Reproduced with permission [34]. Copyright 2021, Elsevier B.V. (b) Azo-linked COF was obtained after the transformation of imine bond through monomer exchange. Reproduced with permission [28]. Copyright 2022, Springer Nature. (c) Azobenzene was introduced into the Azo-COFs skeleton in the form of functionalized monomer, and the photoisomerization under UV irradiation caused the adsorption difference of organic dye molecules. Reproduced with permission [40]. Copyright 2023, Wiley-VCH GmbH.

Azo-CTF by copper-catalyzed oxidative homocoupling reaction of 4,4′,4″-(1,3,5-triazine-2,4,6-triyl)trianiline monomers [34]. Triazine in this structure can be used as a nitrogen-rich center, and azo bond can be used as an active energy storage site in organic electrode materials for LIBs (Fig. 3a). In addition, the porous structures of Azo-CTF provided an open space for lithium ions transmission. The ions transport path is shortened, which is conducive to the redox reaction of the battery. Azo-CTF cathode showed a large and reversible capacity output of 205.6 mAh/g at a current density of 0.1 A/g. However, compared to other types of linkage bonds, the harsh conditions and cumbersome steps of azo bond synthesis may be one of the reasons for the slow development of azo bonded COFs.

Secondly, azo-linkage can be obtained by the conversion of imine linked-COFs. In 2022, Zhao *et al.* treated imine-linked Im-COF-1 with 1,4-dinitrosobenzene under solvothermal conditions, and successfully prepared azo-COF-1 based on azo bonds connection (Fig. 3b) [28]. This method realized the transformation of COFs from –C=N– to –N=N– by changing linking monomers. Moreover, it solved the problem that the azo bond cannot be constructed through conventional monomer condensation due to its low reversibility. The successful formation of an azo bond not only expanded the repertoire of methods and strategies to connect COFs, but also presented a novel approach for synthesizing COFs that were previously challenging to fabricate due to their limited solubility and propensity for fragmentation reactions. In addition, as a bridging functional group, the azo bond exhibits narrow band gap characteristics [35], which has the potential to be used in a variety of applications such as electron transport and redox. However, the number of azo-linked COFs is much less than other types, and more synthetic methods and strategies need to be developed.

Thirdly, azo bonds can be introduced into monomers as functional groups through modification, and then COFs are constructed by other bridging methods. Most of high-performance COFs were obtained by this strategy, *e.g.*, Tp-Azo [36] and NKCOF-47 [37]. It is worth noting that azobenzene is a commonly used photoswitching molecule, and its double bond structure can undergo reversible *E-Z* photoisomerization reaction. After UV irradiation, the structures and properties of the two isomers are quite different, leading to be applied in different fields. Previous studies have reported the synthesis of azobenzene-based photosensitive molecules [38] and its application [39] in the field of wastewater treatment. In 2023, Zhao *et al.* constructed Azo-COFs by condensation of (*E*)-2′-(phenyldiazenyl)-[1,1′:4′,1″-terphenyl]-4,4″-diamine with azobenzene structure and 4-[1,2,2-tris(4-formylphenyl)ethenyl]benzaldehyde (TPE) monomer [40]. The unique porous characteristics of the framework structure provided enough free space for the reversible *trans*-to-*cis* isomerization of azobenzene. After UV irradiation, the *trans* azobenzene exposed to pore space transformed into a *cis* configuration that extends out of the plane of the COFs layer, releasing more pore volume. Thus the diffusion of Light Green SF Yellowish (LGSF) into the pores was favorable and the adsorption capacity of Azo-COFs on LGSF was about 3.7-fold higher (74.78 mg/g) than that without UV irradiation (20.35 mg/g) (Fig. 3c). Luo *et al.* designed D-A (donor-acceptor) system with electron-rich benzene and electron-withdrawing triazine units, and introduced azobenzene in the form of branched chain to obtain ECUT-Azo-COF-1 [41]. After UV irradi-

ation, the isomerization effect of azo bonds increased the absorption capacity of UO_2^{2+} by ECUT-Azo-1 from 220 mg/g to 1380 mg/g, and the yield of hydrogen peroxide in water increased from 62.8 μmol/L to 537.7 μmol/L.

2.1.3. Hydrazone-linked units

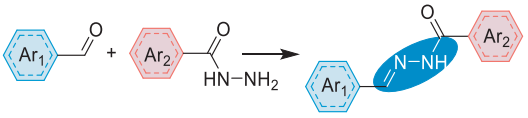

(3)

Hydrazone-linked COFs can be prepared by nucleophilic addition between carbonyl compounds (aldehydes/ketones) and hydrazine (Eq. 3). Compared with imine, hydrazone is more stable and can exist under normal conditions, and has garnered considerable attention in recent years. Wan *et al.* synthesized hydrazone-linked COF-DHz-APS with zwitterion groups under solvent thermal conditions. COF-DHz-APS was melted with Brønsted acid (HA) and then processed into thin films by a simple hot-casting knife method. The porosity and density of these films leads to potential applications in fast ionic conduction and selective separation. Moreover, the structure and crystallinity of COFs were not destroyed, which solves the problem that COFs are powdery and difficult to process (Fig. 4a) [42].

Hydrazone-linked COFs possess multiple active sites and a regular π-conjugated system, thereby facilitating the contact with analytes and exhibiting advantageous signal amplification when utilized in sensing applications. Jiang *et al.* synthesized a Pythz-COF linked by hydrazone using pyrene-based monomer, which exhibited excellent crystallinity and thermal and chemical stability [43]. COFs doped with pyrene elements provided fluorescent channels, so Pythz-COF demonstrated the fluorescence quenching sensing effects toward *p*-nitrophenol, 2,4-dinitrophenol, and 2,4,6-trinitrophenol. In particular, the limit of detection for 2,4,6-trinitrophenol by Pythz-COF was only 0.76 μmol/L. Thus, it is an exceptional cyclic fluorescence sensor material for detecting nitrophenol explosives.

Hydrazone-linked COFs possess a receptor structure (carbonyl group) and have potential application in photocatalytic hydrogen evolution. Tang *et al.* introduced electron-rich conjugated benzotrithiophene (BTT) to prepare BTT-Hz-1 [44]. The hydrazone bond in this structure can be served as anchor site for Pt-species, which was conducive to the photogenerated electron reduction from Pt^{4+} to Pt^0. Subsequently, the electron transfer process from Pt^0 to H^+ yielded final product (H_2). The conjugated BTT structure can broaden the absorption range of visible light and improve the transfer efficiency of photocarriers. In addition, the electron-rich property of BBT contributes to improve the electron-hole separation efficiency. Therefore, BBT-Hz-1 had a high photocatalytic hydrogen evolution rate (17.27 mmol $g^{-1}h^{-1}$).

Modification of hydrazone-linked COFs is considered an effective strategy for optimizing stability, which can be achieved *via* monomer modification and post-treatment of COFs. Wang *et al.* introduced azobenzene groups into the conjugated framework, thereby enhancing the chemical stability of acylhydrazone-connected COFs by promoting π–π packing between adjacent layers [45]. The modified COF-NHU6 exhibited greatly stability in harsh environment, such as in strong acid, strong alkali, and boiling water (even after being exposed to air for one year). In addition, Yang *et al.* prepared a hydrazide-linked COF by oxidizing hydrazone-linked COFs under mild conditions [46]. Compared with before oxidation, the hydrazide-MTH-TFPB COF maintained high crystallinity and porosity even under severe conditions, such as boiling water, strong acids, and strong bases, demonstrating superior chemical stability (Fig. 4b). Furthermore, due to the favorable interactions between iodine molecules and hydrazide functional groups, the adsorption capacity of hydrazide-MTH-TFPB COF for iodine can be increased to 3050 mg/g.

2.2. COFs based on N-containing conjugated rings linkage units

2.2.1. Triazine-linked units

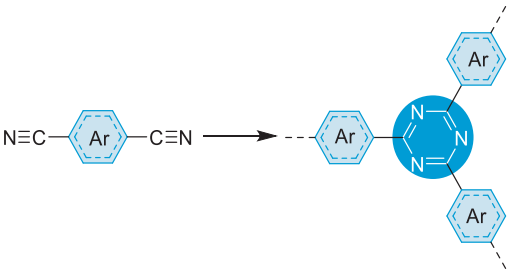

(4)

Generally, covalent triazine frameworks (CTFs) are synthesized through cyclic trimerization of aromatic nitriles (Eq. 4). In 2008, Thomas *et al.* synthesized the first triazine-linked CTF-1 using 1,4-dicyanobenzene as a raw material [47]. Most COFs of this type are catalyzed by $ZnCl_2$ and reacted at 400 °C. Although the structure of the triazine ring is very stable, some products will inevitably decompose at high temperature. Moreover, Zn^{2+} residue exists in the obtained material, which is not conducive to the application of CTFs. Some other synthetic methods also have been developed to construct triazine-linked COFs, such as superacid catalysis [48], amidine-based polycondensation at low temperature [49], P_2O_5 as a catalyst to promote aromatic amide transform into triazine rings [50], and nitrile trimerization routes optimized for polyphosphoric acid ($H_6P_4O_{13}$) [51]. The development of these methods provides feasible mechanisms to synthesize CTFs with diverse structures. In 2023, a method of synthesizing CTFs by cyclotrimerization of aromatic aldehyde was proposed by Jin *et al.* The target products can be obtained under mild reaction condition (160 °C, a small amount of catalyst), and perfluorinated CTF (CTF-TF) can be prepared by this method. The load of H_3PO_4 can be effectively locked upon the interaction of electronegative fluorine site and triazine unit. The proton conductivity of CTF-TF at 150 °C was 1.82×10^{-1} S/cm, which is the highest among the reported CTFs (Fig. 5a) [52]. Xu *et al.* confirmed that crystalline dual-porous pyridinyl CTF (Fe-CTF) with layered structure was successfully synthesized for the first time by using $FeCl_3$-catalyzed polymerization of 2,6-pyridinitrile without solvent. More importantly, $FeCl_3$ can coordinate with pyridine and triazine to form unique Fe-N_3 single-atom active sites. During electrocatalysis, Fe-N_3 can accelerate ORR reaction kinetics, thus improving battery performance [53].

Triazine ring has good conjugation, and its conjugation links with ethylene or benzene ring groups can exhibit great photoelectromagnetic properties. For example, the biphenyl unit in CTF-2 formed a layered micro-mesoporous structure [54], which can enhance the structural stability compared to CTF-1. And it provided a large number of lithium storage active sites. Thus, as an anode, CTF-2 had ultrahigh capacitance (1526 mAh/g at 0.1 A/g), and can be applied to lithium batteries due to the excellent electrochemical performance. Moreover, CTFs can also store K and Na with physical properties similar to Li. Thus, CTFs had great potential application in energy storage devices [55]. In addition, Liu *et al.* obtained a hyperconjugated structure of a TA-Por-sp^2-COF by connecting the porphyrin unit with triazine [56]. The synergistic effect of the electron donor and electron absorbing groups in the hyperconjugated system realized a high photogenerated electron utilization rate. And it had sufficient porosity to provide the reactants for full diffusion; thus, TA-Por-sp^2-COF had good photo-catalytic

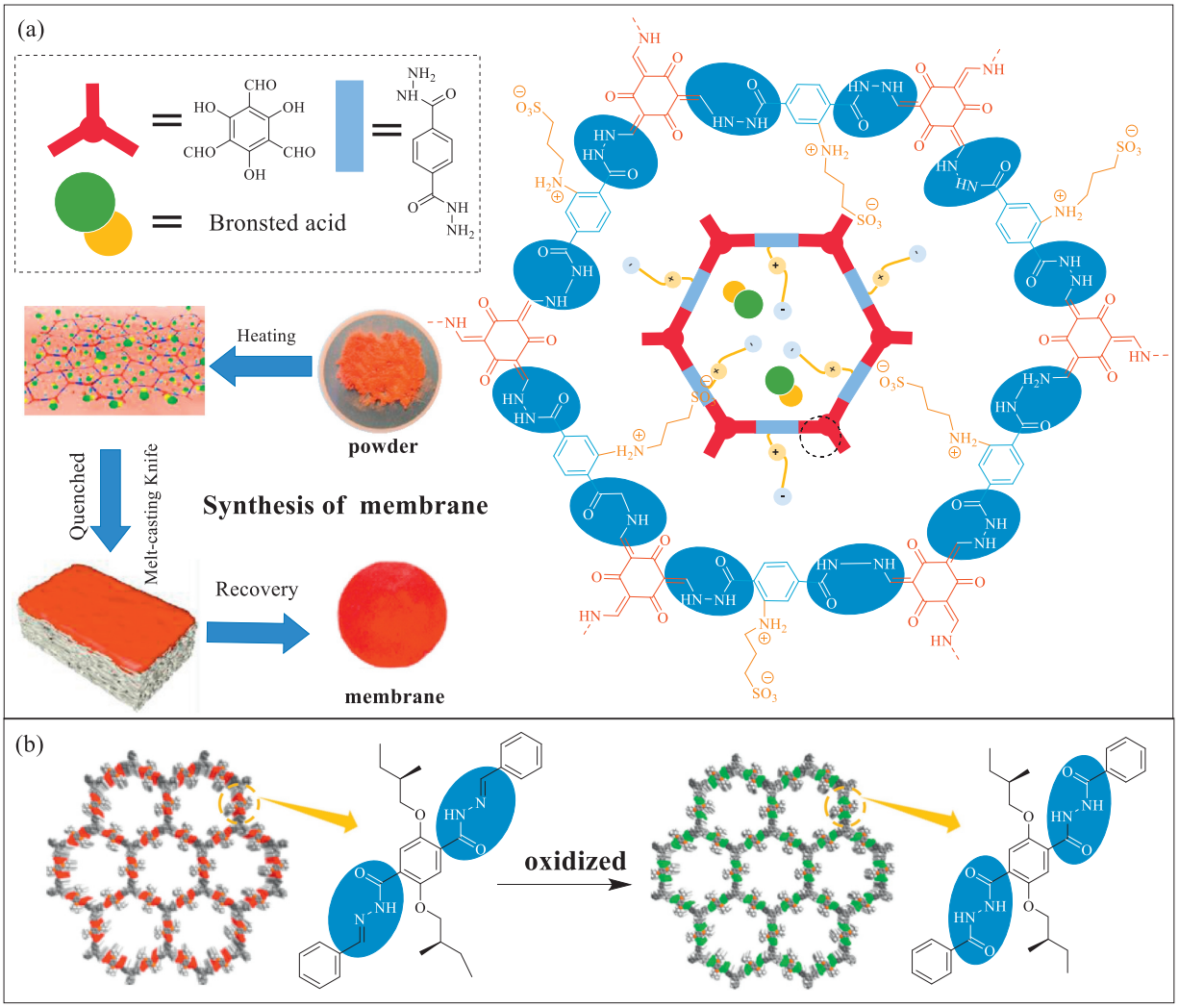

Fig. 4. (a) COF-DHz-APS with APS were melted into film with the action of HA. Reproduced with permission [42]. Copyright 2024, American Chemical Society. (b) The stability of hydrazone-linked TH-TFPB COF was improved after oxidation. Reproduced with permission [46]. Copyright 2022, American Chemical Society.

performance. Benzylamine can be completely reacted by TA-Por-sp^2-COF (as a photocatalyst) within 2 h under white LED irradiation. The selectivity of this reaction was more than 99%, which showed excellent performance in other similar photocatalytic reactions.

Triazine ring is conjugated and nitrogen-rich, which can be utilized as an active site for gas storage or adsorption separation. Zhou *et al.* used 4-acetylbenzonitrile as a two-in-one monomer and trifluoromethanesulfonic acid-catalyzed trimerization to synthesize an aryl-triazine-linked 2D COF, which had good thermal stability and can be used for the adsorption of phenol, bisphenol A, 1-naphthol, and other organic pollutants [57].

2.2.2. Imidazole-linked units

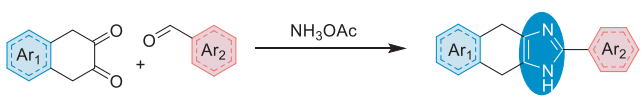

(5)

Imidazole is one of the important structures in N-containing heterocycles. In the past decades, people have explored a variety of imidazole synthesis methods and tried to apply them to the synthesis of imidazole-linked COFs. The common synthetic pathway of imidazole-linked COFs is Debus-Radziszewski reaction. In this reaction process, diketone and ammonia are dehydrated and condensed into diimine, and then condensed with aldehyde to form imidazole ring (Eq. 5). Wang *et al.* synthesized imidazole-linked fully conjugated 3D BUCT-COF-7 through one-pot multicomponent Debus-Radziszewski reaction of the saddle-shaped aldehyde-substituted cyclooctatetrathiophene, pyrene-4,5,9,10-tetraone, and ammonium acetate [58]. BUCT-COF-7 can be used as a metal-free electrocatalyst because of its rich heteroatom and excellent ORR activity. BUCT-COF-7 as cathode catalyst was assembled into the electrolyzer, the electrochemical yield rate of H_2O_2 was as high as 326.9 mmol $g^{-1}h^{-1}$, indicating the potential application of BUCT-COF-7 in energy and environmental catalysis.

On the basis of Debus-Radziszewski synthesis method, Zhang *et al.* proposed an approach of constructing imidazole-linked COFs with multiple monomers (Fig. 5b). The structures of N-substituted imidazolyl COFs can be designed variously by using ammonium acetate, diketone, aldehyde and aromatic amine as raw materials [59]. The synthesized COFs exhibited ultrastability in strong acid and alkali, and the substituent groups can be replaced according to different applications. Under the guidance of this strategy, phosphate-functionalized LZU-530 was synthesized and showed good adsorption capacity for UO_2^{2+} in strong acid environment (95 mg/g, 2 mol/L HNO_3).

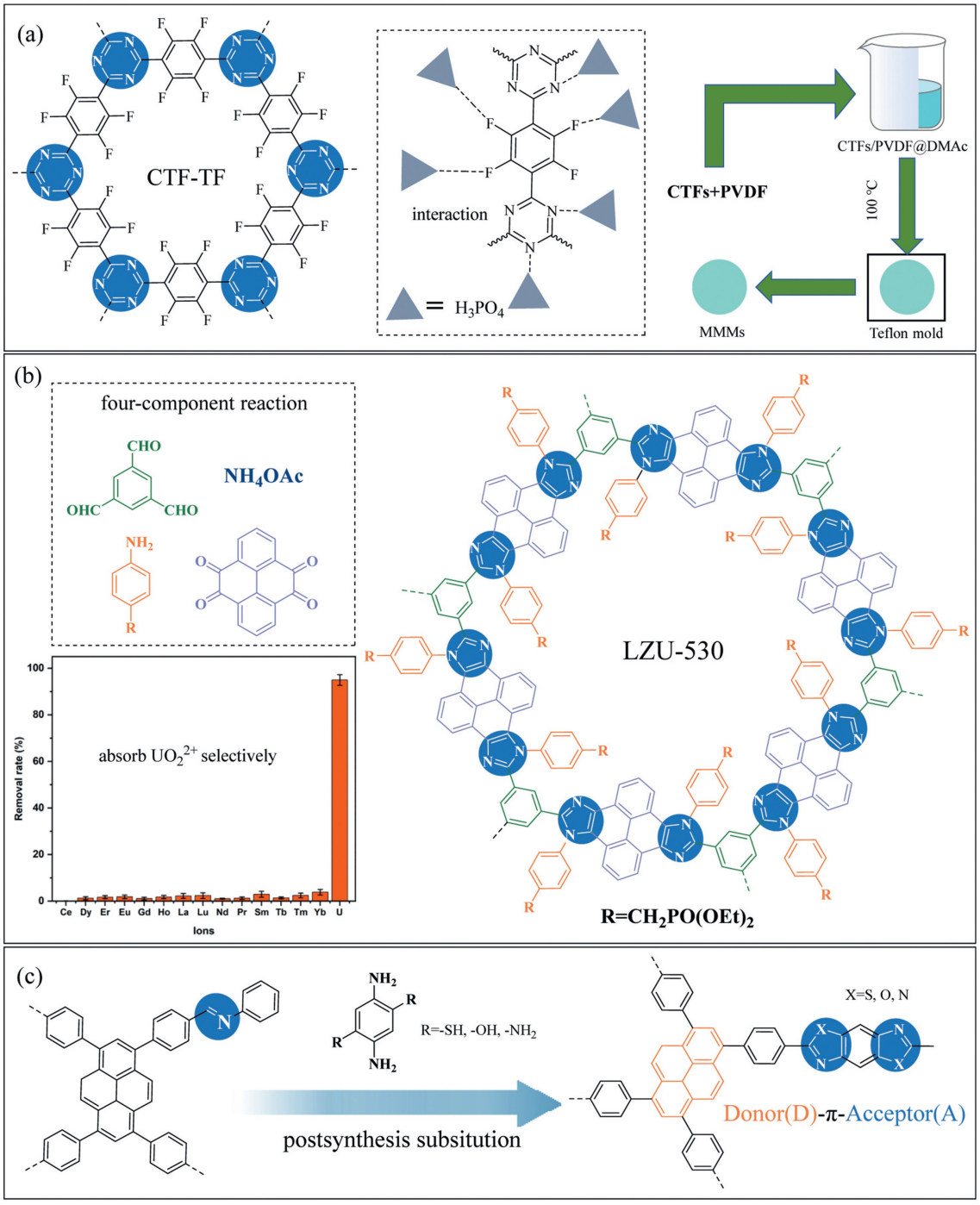

Fig. 5. (a) The perfluorinated CTF-TF loading with H_3PO_4 exhibited high proton conduction abilities. Reproduced with permission [52]. Copyright 2023, Springer Nature. (b) *N*-Substituted imidazoline-linked LZU-530 was synthesized *via* a four-component reaction strategy and selective adsorption of UO_2^{2+} in acid environment. Reproduced with permission [59]. Copyright 2024, American Chemical Society. (c) D-π-A structure was formed by combining pyrene group. Reproduced with permission [62]. Copyright 2023, Wiley-VCH GmbH.

2.2.3. Thiazole-linked units

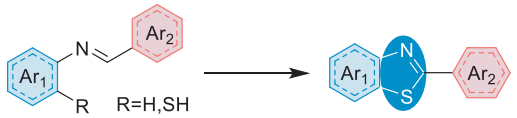

(6)

Thiazole ring can be synthesized in two ways. The first is the reaction between imine bonds and sulphur monomers. The electrophilicity of sp^2-C and the nucleophilicity of S_8 in imines can be used in cascade cycloaddition to obtain thiazoles. The second is that the amino group condenses with aldehyde group and then oxidizes with the adjacent sulfhydryl group to form a ring. The above two methods to obtain thiazole are essentially post-modified cyclization by imine bonds (Eq. 6). In 2018, imide-linked TTT-COF was converted into thiazole-linked TTI-COF by Bettina's team through sulfur-assisted imine bond [60]. The linkage-change from imine to thiazole improved the acid resistance, which provided enlightenment for the synthesis of thiazole-linked COFs. In

2023, Lang *et al.* applied TTT-COF to the photocatalytic oxidation of organic sulfides based on the research result of Bettina [61]. Under blue LED irradiation, methyl phenyl sulfide can be converted into sulfoxide under the action of TTT-COF and TTI-COF, respectively. The conversion rate of methyl phenyl sulfide in TTT-COF was about 8 times that in TTI-COF. Wang *et al.* synthesized three kinds of azoles-linked COFs based on imine-linked ILCOF-1, including thiazole-linked TZ-COF, oxazole-linked OZ-COF and imidazole-linked IZ-COF (Fig. 5c) [62]. D-π-A structure was formed by combining pyrene group with linkage units. This structural feature can effectively promote charge transfer and separation of H^+ from the carrier, thus inhibiting photoexcited charge recombination. Among these three azole structures, thiazole linkage possessed wider visible light absorption, narrower band gap, and more effective electron-hole separation. In the process of photocatalytic production of H_2O_2, the yield of TZ-COF (268 μmol $h^{-1}g^{-1}$) was higher than that of OZ-COF (220 μmol $h^{-1}g^{-1}$) and IZ-COF (120 μmol $h^{-1}g^{-1}$).

2.3. COFs based on N-containing unconjugated rings linkage units

2.3.1. Imide-linked units

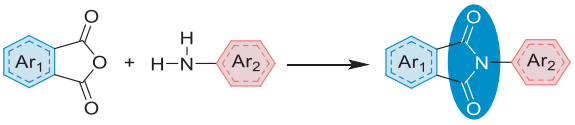

(7)

Imide-linked COFs (PI-COF) can be obtained by the reaction of aromatic dianhydride and triamine (Eq. 7). In 2014, Yan *et al.* employed the solvothermal method to prepare the first imide-connected PI-COF-1 with a pore size of 33 Å. PI-COF-3 with a pore size of 53 Å was prepared by increasing the length of the monomer molecule [63]. Since then, most PI-COFs of this type have been synthesized using solvothermal method. However, the invertibility of the imide bond in the synthesis process is poor, which leads to the difficulty of product crystallization and long reaction time. To solve this problem, Johannes *et al.* proposed the ionothermal synthesis of PI-COFs, where porous PI-COFs were synthesized in the mixture of zinc chloride and eutectic salts at high temperature [64]. Compared with the traditional solvothermal method, the reaction time of the ion thermal method was reduced considerably; however, the reaction process was performed at high temperature. In view of this, in 2022, they also proposed an alcohol-assisted hydrothermal polymerization approach for PI-COFs, which converted imine bonds into imide bonds through ion exchange and realized the conversion between COFs in an environmentally friendly manner [65].

Pyromellitic dianhydride, naphthalene-1,4,5,8-tetracarboxylic acid, and perylene-3,4,9,10-tetracarboxylic dianhydride are the commonly used PI-COF monomers. The combination of monomers with different conjugated structures has a significant influence on the energy storage performance of PI-COFs. Gu *et al.* precisely regulated the size of conjugated units in COFs at the atomic level [66]. They found that the spin density isosurfaces of the imine radical intermediates around single atoms decreased with the increase of conjugated group size. Therefore, the radical electrons can delocalize effectively within the molecule, which enhanced the thermodynamic stability of the imine radical intermediates. Correspondingly, at a current density of 50 mA/g, the capacitance retention of the COF-modified cathode increased from 56% to 96% after 100 cycles. Additionally, Huang *et al.* synthesized imide-linked HAHATN-PMDA-COF using hexa(*p*-anilinyl) hexaazatrinaphthalene and pyromellitic dianhydride. There are two kinds of pores in the structure of HAHATN-PMDA-COF, and their sizes were 1.58 nm and 0.95 nm, respectively. Carbonyl and phenazine units were distributed in these uniform one-dimensional channels, which contributed to the homogeneous deposition of lithium ions, thus improving lithium utilization and stability in battery applications (Fig. 6) [67]. In addition to planar adjustments, 3D spatial adjustments can also change the performance of COFs. Besides, the performance of COFs can be modulated by adjusting 3D spatial structure. In addition, the performance of COFs can be adjusted by adjusting the three-dimensional spatial structure. Wang *et al.* introduced a modulator to adjust the interlayer stacking mode of NKCOF-11 from overlapping (AA) to stagger stacking (ABC) [68]. The absorption capacity of ABC-stacked COFs for ethylene (C_2H_4) or carbon dioxide (CO_2) was increased by 60%. These synthetic strategies provide some inspiration and guidance for COFs structural adjustments.

2.3.2. Other nitrogen-containing rings

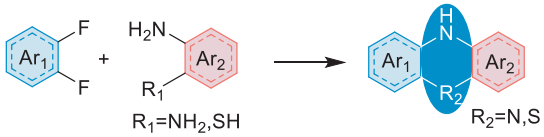

(8)

o-Difluoro can form non-conjugated heterocycles (Eq. 8) by nucleophilic substitution with the amino group on aromatic ring and its neighbouring groups (amine, mercapto, *etc.*). Zeng *et al.* prepared CoPc-DNDS-COF by using 2,5-diaminobenzene-1,4-dithiol monomer [69]. Huang *et al.* synthesized a new piperazine-linked $M_1Pc\text{-}NH_2{-}M_2PcF_8$ *via* nucleophilic substitution reaction between octaminophthalocyanines and hexadecafluorophthalocyanines [70]. Piperazine linkage can be readily oxidized to cationic radicals, leading to the formation of doped COFs with high electrical conductivity. The film sample of $M_1Pc\text{-}NH_2{-}M_2PcF_8$ had high conductivity (12.7 S/m) (Fig. 7).

3. Synthesis of scCOFs

It is of importance to accurately analyze the chemical structure of COFs. It is well known that scCOFs can be characterized by single crystal X-ray diffraction. According to the measured data, we can not only accurately analyze the structure of COFs, but also infer the reasons for its performance. However, for polycrystalline COFs, more characterization methods are needed to indirectly infer the structural characteristics. Therefore, the preparation of scCOFs is beneficial to obtain more accurate structural information and reasonable utilization. At present, preparation of scCOFs mainly includes three methods as follows:

(1) Adding a specific substance as a modulator into the reaction system. The competitive reaction between modulating agent and monomer can reduce the polymerization rate, which contributes to improve crystal defects and obtains high-quality single crystals. In 2016, Bein *et al.* verified that the crystallinity of COF-5-X (X being the functionalized group) can be improved by introducing a modulating agent [71], which provides guidance for the synthesis of scCOFs. In 2018, Yaghi *et al.* developed a method to grow high-quality 3D porous scCOFs using aniline as a modulator [72]. Aniline can decrease the reaction rate of monomer and increase the process of imine exchange, which offered sufficient time for the growth of scCOFs (Fig. 8a). In 2020, Wang *et al.* also used aniline as a modulator to successfully obtain the first non-interpenetrate scCOF (3D LZU-306) [73]. In 2024, acetic acid/aniline was replaced by 2,2,2-trifluoroacetic acid (CF_3COOH)/2,2,2-trifluoroethylamine ($CF_3CH_2NH_2$) in the growth process of single crystal by Wang's

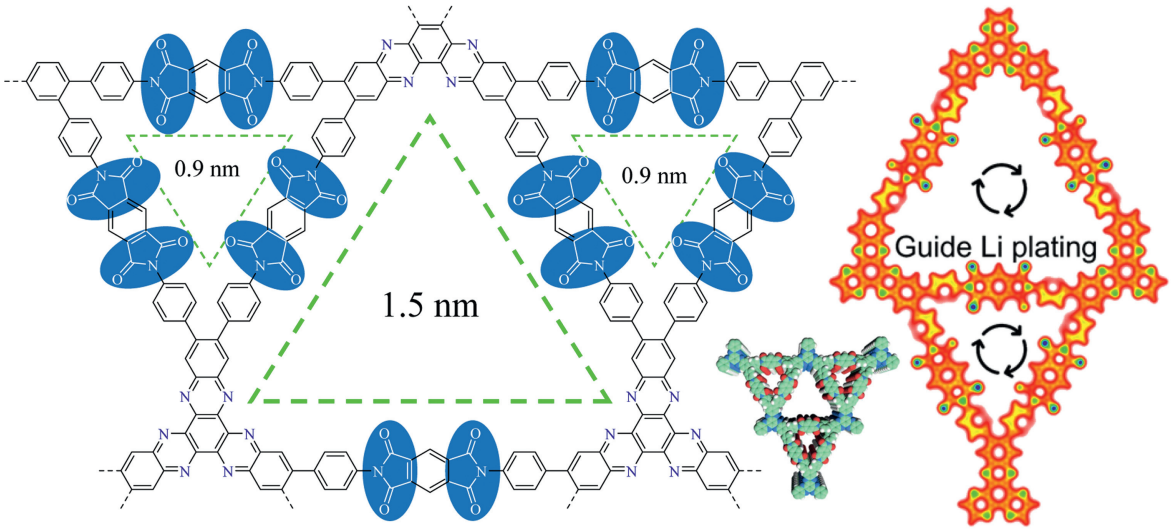

Fig. 6. One-dimensional channels in the two pores promoted the deposition of guided Li. Reproduced with permission [67]. Copyright 2024, Wiley-VCH GmbH.

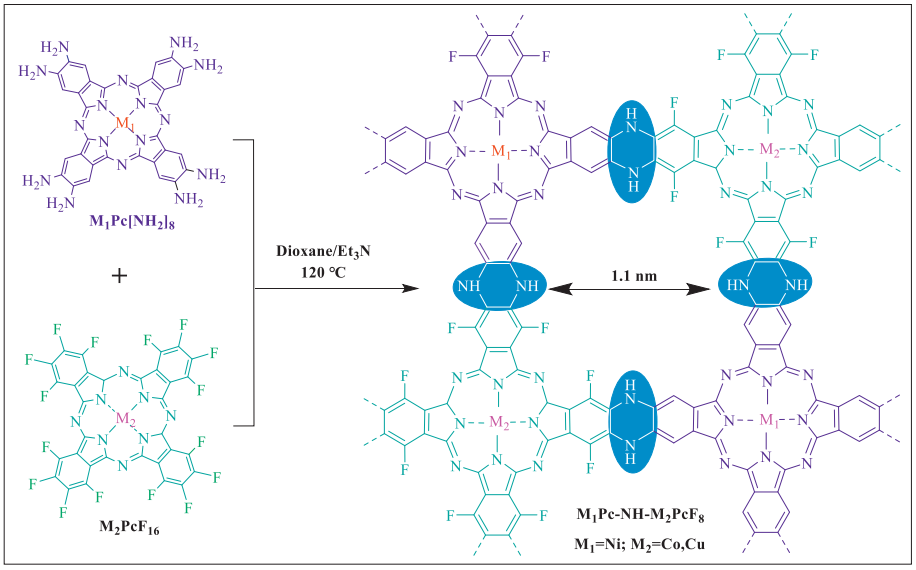

Fig. 7. Synthesis of M_1Pc-NH-M_2PcF_8 COFs through the nucleophilic substitution reaction. Reproduced with permission [70]. Copyright 2022, American Chemical Society.

team, and the growth of scCOFs can be completed within 1–2 days [74].

(2) Controlling the growth condition and rate of crystal nucleus by adjusting the solvent conditions. In 2019, Dichtel *et al.* revealed that the boronate ester-linked COFs can be transformed into single crystals structure by adding nitrile-containing cosolvents [75]. Wei *et al.* controlled the crystallization kinetics by adding supercritical CO_2 (sc-CO_2), which effectively accelerated the synthesis process (Fig. 8b) [76]. Borate-linked COF-5 can be prepared within 2–5 min by this way. In 2023, Zheng *et al.* used amphiphilic amino-acid derivatives with long hydrophobic chains to self-assemble into micelles. Hydrophobic compartments were formed inside the micelles, which were able to separate different monomers according to the solubility differences of substances. This strategy avoids the precipitation phenomenon caused by irregular binding between monomers and thus regulating the orderly crystallization process of molecules [77].

(3) Transformation from single crystal to single crystal (SCSC). In 2023, Jiang *et al.* constructed USTB-5 single crystal by using tetraphenylmethane monomer. The imine linkage bond in the structure was reduced to amine through degassing of USTB-5 single crystal, and a new USTB-5r single crystal was obtained. In addition, the imine bond in USTB-5 can also be oxidized into an amide bond by sodium chlorite to obtain a new USTB-5o single crystal (Fig. 8c) [78].

4. Potential application of COFs in environmental field

Nitrogen plays an important role in wastewater treatment. Activated carbon, zeolite and other water purification materials often need to be modified to introduce some active sites such as N, S and O to improve the purification capacity. NCLB-COFs contains nitrogen and other heteroatoms, which can provide abundant active sites. Combined with the porous characteristics, NCLB-COFs can detect, adsorb or degrade pollutants. Therefore, NCLB-COFs has advantages in wastewater treatment [79].

Coordination mechanism is a common strategy to adsorb heavy metal ions or organic pollutants. The rich porous structure of NCLB-COFs ensures that pollutants in water can fully diffuse into the material. And then the pollutants can be coordinated, captured and locked by nitrogen and other heteroatom [80]. Adsorbents

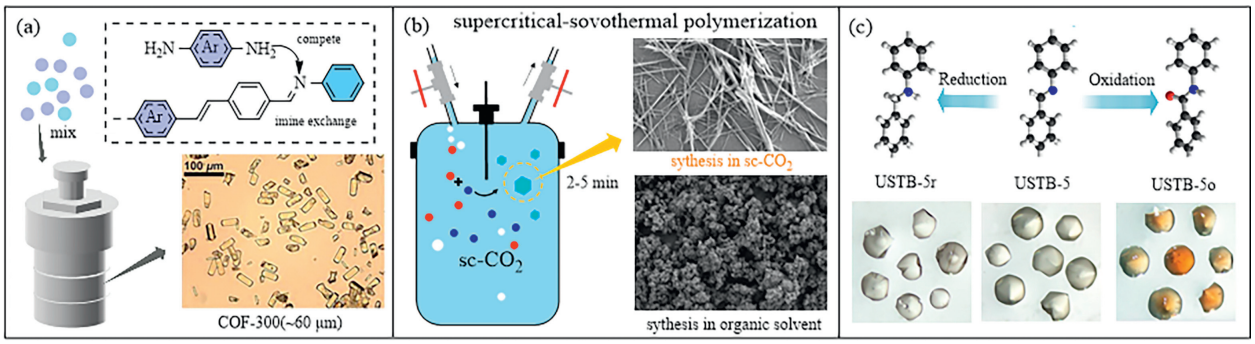

Fig. 8. (a) A modulator was added to the reaction system to decrease the reaction speed and improve the crystal quality. Reproduced with permission [72]. Copyright 2018, the American Association for the Advancement of Science. (b) sc-CO_2 accelerated the reaction process and produced crystals quickly. Reproduced with permission [76]. Copyright 2021, Springer Nature. (c) Linkage changes undergo SCSC transformation. Reproduced with permission [78]. Copyright 2023, Springer Nature.

with coordination mechanism were highly favored, because the coordination process is reversible. Therefore, the adsorbed pollutants can be released from NCLB-COFs without changing the structure, thus realizing the absorption/desorption cycle. Additionally, COFs with photocatalytic properties can be obtained by introducing specific activity or reasonably designing D-A (donor-acceptor) structure, which can photodegrade harmful pollutants and transform them into harmless substances [81,82]. Moreover, the specified organic pollutants can be quantitatively detected by introducing photothermal reactive groups into the COFs structure [83-85]. Therefore, NCLB-COFs has a significant application prospect in environmental treatment.

5. Conclusions and prospects

The geometry and spatial arrangement of the COFs is largely determined by the connection methods of nodes and the symmetry of the molecular structure. The skeleton and structural properties of COFs are closely related to the composition and classes of chemical bonds. The majority of COFs were constructed following the bottom-up strategy, that is, starting from monomer molecules and then building rings by bridging functional groups. The development of COFs linked by common nodes is often limited by some objective factors (such as the solubility of ligand molecules or the specificity of reaction products). Therefore, some new synthetic methods (such as the synthesis of COF-B by exchanging the "parts" of the COF-A skeleton) have been developed. At present, the chemical bonds of the reported COFs are mostly reversible, which can make the molecules constantly self-repair (formation-fracture-regeneration) during ring formation, and finally form a highly crystalline structure. Additionally, there are also a few COFs constructed by irreversible covalent bonds, which use the rigidity of the structural units and the orientation of the chemical bonds in linkage nodes to promote the crystallization of the molecules. In a word, the diversified synthesis strategies can provide significant references for the development of new COFs.

Despite the remarkable progress in the research of COFs, some challenges still need to be overcome for future applications. (1) Exploring new molecular modules and developing novel linked-bonds to meet different application requirements are still the center driver for the development of COFs. Based on the reported synthesis methods (such as click chemistry), we should further explore the economic, simple preparation methods of COFs. (2) The combination of theoretical calculation and artificial intelligence for COFs research is still at early stage. It is necessary to establish more systematic theoretical algorithms, rich databases and appropriate evaluation methods to strengthen the theoretical research of COFs and optimize the synthesis of COFs. (3) The poor machinability of powdered COFs hinders its development of industrial and commercial applications. It is still necessary to explore the material forming process suitable for mass production to improve the practicability of COFs.

To sum up, we summarize the research progress of NCLB-COFs in recent years. We hope that this review can provide beneficial guidance for studying the synthesis and properties of COFs. We believe that the research of COFs will achieve more outstanding progress in the near future through the continuous efforts of researchers.

Declaration of competing interest

The authors declare that they have no known competing financial interests or personal relationships that could have appeared to influence the work reported in this paper.

CRediT authorship contribution statement

Liying Ou: Writing – original draft, Validation, Software, Resources, Investigation, Formal analysis, Data curation. **Zhenluan Xue:** Writing – review & editing, Supervision, Investigation, Funding acquisition. **Bo Li:** Writing – review & editing, Visualization, Funding acquisition, Conceptualization. **Zhiwei Jin:** Validation, Software, Formal analysis. **Jiaochan Zhong:** Validation, Software. **Lixia Yang:** Validation, Software, Formal analysis. **Penghui Shao:** Writing – review & editing, Resources, Funding acquisition, Conceptualization. **Shenglian Luo:** Supervision, Funding acquisition, Conceptualization.

Acknowledgments

This study was financially supported by the National Key Research and Development Program of China (Nos. 2022YFD1700800 and 2023YFC3905903), the Science and Technology Project of Education Department of Jiangxi Province (No. GJJ2201103), the Fund of Nanchang Hangkong University (Nos. EA202201110 and EA202201065) and National Undergraduate Innovation and Entrepreneurship Training Program (No. 202310406023) the National Natural Science Foundation of China (No. 52470149).

Supplementary materials

Supplementary material associated with this article can be found, in the online version, at doi:10.1016/j.cclet.2024.110294.

References

[1] A.P. Côté, A.I. Benin, N.W. Ockwig, et al., Science 310 (2005) 1166–1170.
[2] D.S. Zhen, C.L. Liu, Q.H. Deng, et al., Chin. Chem. Lett. 35 (2024) 109249.

[3] T. Wang, X. Yu, Y.Q. Xie, Chin. Chem. Lett. 35 (2024) 109320.
[4] G.R. Li, Y.J. Wu, C. Zhong, et al., Chin. Chem. Lett. 35 (2024) 108904.
[5] Y.Y. Zhao, C.T. Yang, Y.J. Yu, Chin. Chem. Lett. 35 (2024) 108865.
[6] M.X. Wu, Y.W. Yang, Chin. Chem. Lett. 28 (2017) 1135–1143.
[7] N. Huang, P. Wang, D.L. Jiang, Nat. Rev. Mater. 1 (2016) 16068.
[8] D.L. Cui, D.F. Perepichka, J.M. MacLeod, et al., Chem. Soc. Rev. 49 (2020) 2020–2038.
[9] J.H. Chang, F.Q. Chen, H. Li, et al., Nat. Commun. 15 (2024) 813.
[10] Z.T. Wang, Y.J. Huang, New J. Chem. 47 (2023) 3668–3671.
[11] Q. Ma, X.Y. Liu, J. Qian, et al., Sep. Purif. Technol. 323 (2023) 124368.
[12] C. Qian, L.L. Feng, W.L. Teo, et al., Nat. Rev. Chem. 6 (2022) 881–898.
[13] Q.B. Fu, T.T. Zhang, X. Sun, et al., Chem. Eng. J. 454 (2023) 140154.
[14] W.B. Dong, Z.Y. Qin, K.X. Wang, et al., Angew. Chem. Int. Ed. 62 (2022) e202216073.
[15] Y.P. Cheng, J.J. Xin, L.B. Xiao, et al., J. Am. Chem. Soc. 145 (2023) 18737–18741.
[16] L. Hao, K.H. Huang, N.X. Wang, et al., Dalton Trans. 51 (2022) 14952–14959.
[17] G.B. Wang, H.P. Xu, K.H. Xie, et al., J. Mater. Chem. A 11 (2023) 4007–4012.
[18] X.L. Fu, Z. Lu, H.J. Yang, et al., J. Polym. Sci. 59 (2021) 2036–2044.
[19] D.W. Burke, R.R. Dasari, V.K. Sangwan, et al., J. Am. Chem. Soc. 145 (2023) 11969–11977.
[20] S.H. An, X.W. Li, S.S. Shang, et al., Angew. Chem. Int. Ed. 62 (2023) e202218742.
[21] J. You, F. Yuan, S.S. Cheng, et al., Chem. Mater. 34 (2022) 7078–7089.
[22] C.J. Kang, Z.Q. Zhang, S. Kusaka, et al., Nat. Mater. 22 (2023) 636–643.
[23] R. Bao, Z.H. Xiang, Z.L. Qiao, et al., Angew. Chem. Int. Ed. 62 (2023) e202216751.
[24] J.H. Ding, X.Y. Guan, J. Lv, et al., J. Am. Chem. Soc. 145 (2023) 3248–3254.
[25] R.Y. Liu, K.T. Tan, Y.F. Gong, et al., Chem. Soc. Rev. 50 (2021) 120–242.
[26] W.Q. Wang, D.K. Huang, W.L. Zheng, et al., Chem. Mater. 35 (2023) 7154–7163.
[27] Z.W. Lu, C.Y. Yang, L. He, et al., J. Am. Chem. Soc. 144 (2022) 9624–9633.
[28] Z.B. Zhou, P.J. Tian, J. Yao, et al., Nat. Commun. 13 (2022) 2180.
[29] Y.L. Yang, L. Yu, T.C. Chu, et al., Nat. Commun. 13 (2022) 2615.
[30] X.L. Li, C.L. Zhang, S.L. Cai, et al., Nat. Commun. 9 (2018) 2998.
[31] L. Cusin, H. Peng, A. Ciesielski, et al., Angew. Chem. Int. Ed. 60 (2021) 14236–14250.
[32] Y.Q. Zhu, D.K. Huang, W.Q. Wang, et al., Angew. Chem. Int. Ed. 63 (2024) e202319909.
[33] Z.B. Zhou, H.H. Sun, Q.Y. Qi, et al., CCS Chem. 6 (2024) 2230–2240.
[34] C.G. Wu, M.J. Hu, X.R. Yan, et al., Energy Storage Mater. 36 (2021) 347–354.
[35] H. Fliegl, A. Köhn, C. Hättig, et al., J. Am. Chem. Soc. 125 (2003) 9821–9827.
[36] M.K. Hota, S. Chandra, Y.J. Lei, et al., Adv. Funct. Mater. 32 (2022) 22011.
[37] S.P. Jia, L.Q. Hao, Y.J. Liu, et al., ACS Mater. Lett. 5 (2023) 458–465.
[38] D. Fang, Z.Y. Zhang, Z.C. Shangguan, et al., J. Am. Chem. Soc. 143 (2021) 14502–14510.
[39] J. Gemen, J.R. Church, T.-P. Ruoko, et al., Science 381 (2023) 1357–1363.
[40] Y.L. Zhao, X.F. Tao, J.P. Lin, et al., Adv. Funct. Mater. 33 (2023) 2302225.
[41] L.C. Guo, Y.T. Yang, L.L. Gong, et al., Adv. Funct. Mater. 36 (2024) 2674–2684.
[42] X.L. Gu, L.Y. Zhao, J. Sun, et al., Chem. Mater. 36 (2024) 2674–2684.
[43] S. Jiang, L.C. Meng, M.X. Lv, et al., Microporous Mesoporous Mater. 348 (2023) 112405.
[44] Q.Q. Tang, Y.Y. Gu, J. Ning, et al., Chem. Eng. J. 470 (2023) 144106.
[45] Y.L. Zhao, Y. Zhao, C.L. Wu, et al., Chem. Eur. J. 27 (2021) 9391–9397.
[46] Y.X. Yang, X.H. Tang, J.L. Wu, et al., ACS Appl. Polymer. Mater. 4 (2022) 4624–4631.
[47] P. Kuhn, M. Antonietti, A. Thomas, Angew. Chem. Int. Ed. 47 (2008) 3450–3453.
[48] S.J. Ren, M.J. Bojdys, R. Dawson, et al., Adv. Mater. 24 (2012) 2357–2361.
[49] K.W. Wang, L.M. Yang, X. Wang, et al., Angew. Chem. Int. Ed. 56 (2017) 14149–14153.
[50] S.-Y. Yu, J. Mahmood, H.-J. Noh, et al., Angew. Chem. Int. Ed. 57 (2018) 8438–8442.
[51] T. Sun, Y. Liang, W.J. Luo, et al., Angew. Chem. Int. Ed. 61 (2022) e202203327.
[52] L.J. Guan, Z.Q. Guo, Q. Zhou, et al., Nat. Commun. 14 (2023) 8114.
[53] K. Cui, X.L. Tang, X.P. Xu, et al., Angew. Chem. Int. Ed. 63 (2024) e202317664.
[54] F. Jiang, Y.J. Wang, T.P. Qiu, et al., J. Power Sources 523 (2022) 231041.
[55] P. Xiong, S.L. Zhang, R. Wang, et al., Energy Environ. Sci. 16 (2023) 3181–3213.
[56] X.X. Liu, R.L. Qi, S.M. Li, et al., J. Am. Chem. Soc. 144 (2022) 23396–23404.
[57] C.D. Zhou, H.Y. Zhou, S.Y. Tang, et al., Mater. Lett. 332 (2023) 133493.
[58] Y.T. Zhang, Z.L. Qiao, R. Zhang, et al., Angew. Chem. Int. Ed. 62 (2023) e202314539.
[59] Z.C. Zhang, P.L. Wang, Y.F. Sun, et al., J. Am. Chem. Soc. 146 (2024) 4822–4829.
[60] F. Haase, E. Troschke, G. Savasci, et al., Nat. Commun. 9 (2018) 2600.
[61] Y.X. Wang, F.W. Huang, W.L. Sheng, et al., Appl. Catal. B 338 (2023) 123070.
[62] Y. Mou, X.D. Wu, C.C. Qin, et al., Angew. Chem. Int. Ed. 62 (2023) e202309480.
[63] Q.R. Fang, Z.B. Zhuang, S. Gu, et al., Nat. Commun. 5 (2014) 4503.
[64] J. Maschita, T. Banerjee, G. Savasci, et al., Angew. Chem. Int. Ed. 59 (2020) 15750–15758.
[65] J. Maschita, T. Banerjee, B.V. Lotsch, Chem. Mater. 34 (2022) 2249–2258.
[66] S. Gu, X.X. Ma, J.J. Chen, et al., J. Energy Chem. 69 (2022) 428–433.
[67] X.Y. Wu, S.Q. Zhang, X.Y. Xu, et al., Angew. Chem. Int. Ed. 63 (2024) e202319355.
[68] Z.F. Wang, Y.S. Zhang, T. Wang, et al., Small 19 (2023) 2303684.
[69] X.B. Yang, X.W. Li, M.H. Liu, et al., ACS Mater. Lett. 5 (2023) 1611–1618.
[70] Y. Yue, H.Y. Li, H.Z. Chen, et al., J. Am. Chem. Soc. 144 (2022) 2873–2878.
[71] M. Calik, T. Sick, M. Dogru, et al., J. Am. Chem. Soc. 138 (2016) 1234–1239.
[72] T. Ma, E.A. Kapustin, S.X. Yin, et al., Science 361 (2018) 48–52.
[73] L. Liang, Y. Qiu, W.D. Wang, et al., Angew. Chem. Int. Ed. 59 (2020) 17991–17995.
[74] J. Han, J. Feng, J. Kang, et al., Science 383 (2024) 1014–1019.
[75] A.M. Evans, I. Castano, A. Brumberg, et al., J. Am. Chem. Soc. 141 (2019) 19728–19735.
[76] L. Peng, Q.Y. Guo, C.Y. Song, et al., Nat. Commun. 12 (2021) 5077.
[77] Z.P. Zhou, L. Zhang, Y.H. Yang, et al., Nat. Chem. 15 (2023) 841–847.
[78] B.Q. Yu, R.B. Lin, G. Xu, et al., Nat. Chem. 16 (2024) 114–121.
[79] Z.L. Zhou, Y.T. Xiao, J. Tian, et al., J. Mater. Chem. A 11 (2023) 3245–3261.
[80] D.C. Mei, L.J. Liu, B. Yan, Coord. Chem. Rev. 475 (2023) 214917.
[81] H.R. Zhang, L. Zhang, S.S. Dong, et al., J. Hazard. Mater. 446 (2023) 130756.
[82] S.P. Qi, R.T. Guo, Z.X. Bi, et al., Small 19 (2023) 2303632.
[83] W.Z. She, C.H. Li, R.S. Li, et al., Sep. Purif. Technol. 330 (2024) 125294.
[84] Y.X. Yu, Q.Q. Jin, Y.B. Ren, et al., Chem. Eng. J. 465 (2023) 142819.
[85] Z.C. Xiao, X.Y. Nie, Y. Li, et al., ACS Appl. Mater. Interfaces 15 (2023) 9524–9532.